REVIEW

Photoinduced Electron-Transfer Processes in Fullerene-Based Donor–Acceptor Systems

by **K. George Thomas*** and **Manapurathu V. George***

Division of Photosciences and Photonics, Regional Research Laboratory, Trivandrum 695 019, India (e-mail: kgt@vsnl.com (K. George Thomas), mvgeorge@rediffmail.com (M. V. George))

and

Prashant V. Kamat*

Radiation Laboratory, University of Notre Dame, Notre Dame, IN 46556, USA (e-mail: kamat@hertz.rad.nd.edu)

Dedicated to Professor Dr. *Rolf Huisgen* on his 85th birthday. One of the authors (*M. V. G.*) spent a year (1961) with Professor *Huisgen* at the Institut für Organische Chemie, Universität München as an *Alexander von Humboldt* post-doctoral fellow initially and later visited him several times. He is grateful to Professor *Huisgen* for the constant support and encouragement.

Photoinduced electron-transfer processes in fullerene-based donor–acceptor dyads (D–B–A) in homogeneous and cluster systems are summarized. Stabilization of charge has been achieved through the use of fullerene substituted-aniline/heteroaromatic dyads with tunable ionization potentials and also by using fullerene clusters. The rate constants for charge separation (k_{CS}) and charge recombination (k_{CR}) in fullerene substituted-aniline/heteroaromatic dyads show that forward electron transfer falls in the normal region of the *Marcus* curve and the back electron transfer in the inverted region of the *Marcus* parabola. Clustering of fullerene-based dyads assists in effective delocalization of the separated charge and thereby slows down the back electron transfer in these cases.

Introduction. – Photoinduced electron-transfer processes play a very dominant role in several natural systems. In the photosynthetic systems, for example, the primary process involves the transfer of an electron, on absorption of light, from a donor center to an acceptor site, such that there is efficient charge separation, once the electron has been transferred [1]. A simplified picture of some of the processes taking place in a donor–bridge–acceptor (D–B–A) system, on absorption of light is shown in the *Scheme*. In this case the donor group (D) is covalently linked to an acceptor group (A) through either a rigid or flexible bridging unit (B). Photoexcitation of either the donor or acceptor would result in an excited state, followed by electron transfer leading to charge-separated species. Stabilization of the charge-separated species by preventing the back electron transfer is important for the successful use of such molecular systems for energy-conversion devices and related applications. The major factors, which control electron transfer, include energetics of the donor and acceptor, distance and orientation between the donor and acceptor, and the nature of the bridging unit.

Several strategies have been adopted for the design of D–B–A systems, which can generate charge–separated states with high efficiency and slow charge recombination

Scheme

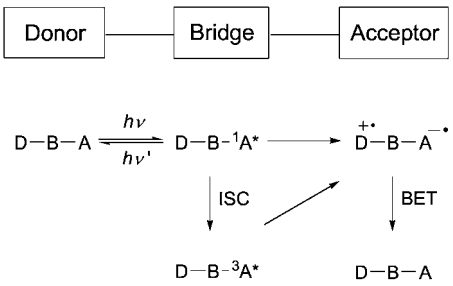

[2]. In the case of natural photosynthetic systems, one of the important factors responsible for the high efficiency of electron transfer is the well-defined orientations of various chromophoric groups in the protein matrices [1].

Recent studies have shown that fullerene C_{60} is an excellent acceptor for the design of D–B–A systems [3]. Photoinduced charge-transfer processes in fullerene-based dyads and triads have received considerable attention [4–15]. In these cases, the singlet or triplet excited state of the photoexcited C_{60} accepts an electron from the linked donor group to give the charge-separated state. Several fullerene-based donor acceptor systems containing porphyrins [7–9][12], phthalocyanines [10], ruthenium complexes [7b][11], ferrocenes [12], and anilines [8a][14][15] as donors have been examined to study the photoinduced charge separation in these dyads. The present article is a brief review of some of the results of our studies on photoinduced electron transfer in fullerene-based dyads.

Donor–Bridge–Acceptor Systems. – A major objective has been the design and study of some fullerene-based D–B–A systems, which can generate long-lived charge-separated states, on photoexcitation. In this context, attention was focused on three related aspects. These include *i*) the design of fullerene-based D–B–A systems to examine the rate and efficiency of electron transfer as a function of distance and orientation, *ii*) the design of fullerene-based D–B–A systems to examine the effect of the redox properties of the donor in the charge-separation processes, and *iii*) photoinduced electron transfer in clusters of fullerene-based systems.

Some of the representative examples of the fullerene-based D–B–A systems that were studied include the pyrrolidino-fullerene-bridged-aniline dyads **1** and **2** [15]. The dyads **1** and **2** enable one to examine the orientation effects in electron transfer in a set of fullerene based D–B–A systems. The difference in orientation is achieved by attaching the aniline donor to the *ortho*- as well as *para*-positions of the phenyl groups of fullereno(1-methyl-2-phenylpyrrolidine) linked by CH_2 chains. *N*-Methylfullerono-pyrrolidine **3**, reported in the literature [4][12], was used for comparison.

Fullerene–Aniline Dyads. – The strategy adopted for the synthesis of **1** and **2** involved the cycloaddition of the appropriate azomethine ylides to one of the reactive C=C bonds of fullerene (between two six-membered rings) [15].

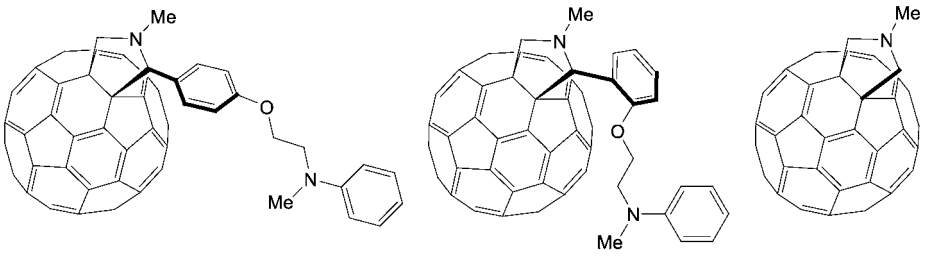

1 **2** **3**

The geometries of the different conformers of **1** and **2** were evaluated by the *Sybyl* force-field method [16]. Computational studies suggest that the most-stable conformation in the case of the *para*-substituted dyad **1** is the extended one, while the *ortho*-subsituted dyad **2** possesses the folded conformation. The energy-minimized structures of **1** and **2** are displayed below. Based on calculations, the edge to edge distance between the aniline N-atom and C_{60} is found to be much larger (9.48 Å) for the *para*-substituted compound **1** than the *ortho*-substituted compound **2** (3.28 Å).

The photoinduced charge-transfer processes in the dyads **1** and **2** were studied by estimating the rate constants for charge separation, and its efficiency using steady-state and time-resolved techniques.

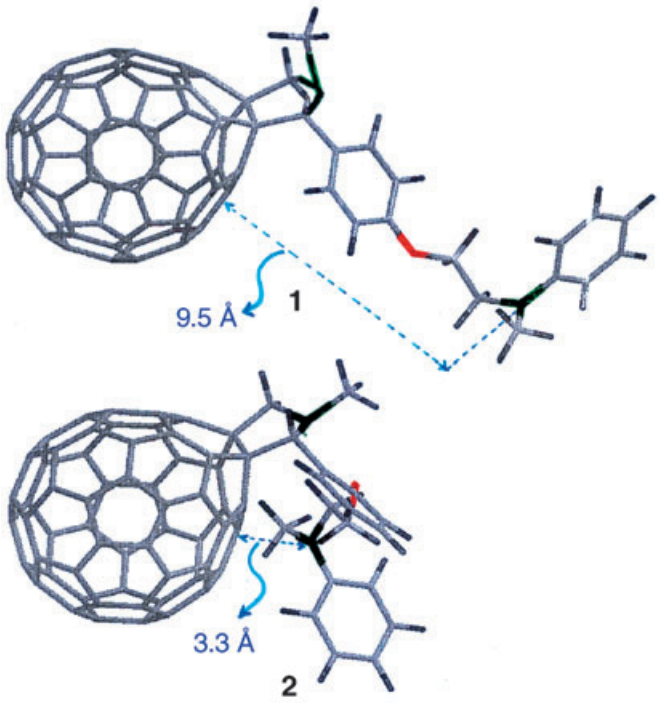

The absorption spectra of the dyads **1** and **2** are very similar to the spectrum of a model fullerenopyrrolidine derivative **3**, but distinctly different from that of pristine C_{60}. The model compound **3** possesses a long-wavelength band around 700 nm. In the case of the dyads **1** and **2**, a weak charge-transfer band is also merged in this 700-nm band, which results from the ground-state interaction between the lone pair of the aniline N-atom and the fullerene π-electron system. This is indicated clearly in the absorption spectrum of the dyad **2** shown in *Fig. 1*. Dyad **2** possesses a long-wavelength band around 702 nm in CH_2Cl_2 (*a* in the *Inset*, *Fig. 1*).

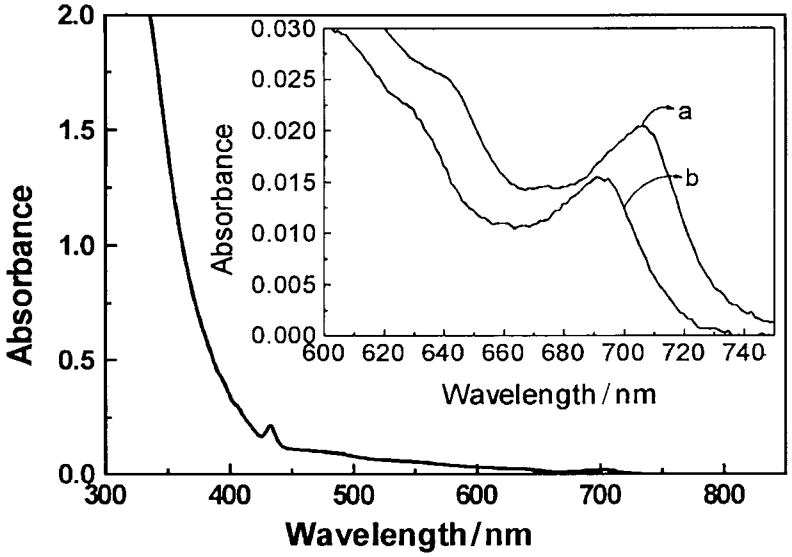

Fig. 1. *Absorption spectrum of the dyad* **2** *in* CH_2Cl_2. *Inset:* Effect of TFA, [TFA] (*a*) 0 and (*b*) 25 mM.

A hypsochromic shift of nearly 14 nm is observed in the long-wavelength band, on adding 25 mM CF_3COOH (TFA) (*b* in the *Inset*, *Fig. 1*). This change can be completely reversed by adding 30 mM of pyridine. These results indicate the possibility of ground-state electronic interaction between C_{60} and aniline in dyad **2** as the protonation of the N-atom inhibits such a charge-transfer interaction. In the case of **3**, the spectrum remains unaffected even after adding 250 mM of TFA.

The fluorescence properties of the dyads **1** and **2** were investigated in solvents of varying polarity. The fluorescence spectral profile and the quantum yields of **1** and **2**, and the model compound **3** were found to be nearly identical in a nonpolar solvent such as toluene, indicating the absence of an electron transfer quenching in the excited state. However, a decrease in the quantum yield of fluorescence was observed for both **1** and **2** with increase in solvent polarity. In a polar solvent such as benzonitrile, a marked decrease in the fluorescence yield was observed. This was particularly significant for the *ortho*-substituted compound **2.** The rate constant and quantum yield of charge separation (k_{CS} and ϕ_{CS}, resp.) *via* the excited singlet state of dyads **1** and **2** were

estimated from the corresponding quantum yield and the lifetime of the model compound **3**. These are summarized in *Table 1*.

Table 1. *Fluorescence Quantum Yields* (ϕ_f), *Rates of Charge Separation* (k_{CS}), *and Quantum Yields* (ϕ_f) *of Charge Separation for Dyads* **1** *and* **2**

Solvent	**1**		**2**	
	ϕ_f [10^{-4}]	k_{CS} [10^9 s^{-1}]^a) (ϕ_{CS})^b)	ϕ_f [10^{-4}]	k_{CS} [10^9 s^{-1}]^a) (ϕ_{CS})^b)
Toluene ($\varepsilon = 2.38$)	6.8		6.7	
CH_2Cl_2 ($\varepsilon = 8.93$)	3.3	0.64 (45%)	1.7	2.0 (72%)
Benzonitrile ($\varepsilon = 25.20$)	3.1	1.11 (49%)	0.83	4.9 (86%)

^{a}) $k_{CS} = [(\phi_{ref}/\phi_f) - 1]1/\tau_{ref}$. ^{b}) $\phi_{CS} = k_{CS}/[(1/\tau_{ref}) + k_{CS}]$.

Excited-State Interactions. – Picosecond-laser-flash photolysis experiments were performed with 355-nm laser pulses from a mode-locked, *Q*-switched *Quantel YG-501 DP Nd:YAG* laser system (output 1.5 mJ/pulse; pulse width *ca.* 18 ps) [17]. The time-resolved absorption spectra of the fullerene–aniline dyad **1**, for example, showed the formation of the singlet excited state with a broad absorption maximum in the region of 890 nm. As the singlet excited state decayed, a new absorption maximum corresponding to the triplet excited state appeared in the region of 690–700 nm. From the rate of decay of the absorption around 890 nm, it was possible to evaluate the lifetime of the singlet state of **1** as 1.05 ns. It may be mentioned that the excited singlet state of pristine C_{60} shows an absorption maximum at 920 nm with a lifetime of 1.2 ns.

The triplet state of the dyad **1**, for example, is characterized by two absorption maxima at 370 and 700 nm. The lifetime of the triplet state of **1** was found to be around 7 μs in benzonitrile. This lifetime is much shorter than the one reported for C_{60}, which is of the order of 100 μs. The reduced lifetime of the triplet of **1** suggests quenching of the photoexcited moiety by the covalently attached aniline group. While the triplet quantum yield of the model fullereno-pyrrolidine **3** is similar to that of pristine C_{60} ($\phi = 0.95$), the triplet quantum yield of **1** is nearly 30% smaller. The lower triplet quantum yield of **1** suggests that the intramolecular quenching of the singlet excited state is a competing process to the intersystem crossing.

Efficiencies in Electron-Transfer Processes. – The photosynthetic process that occurs in nature involves a sequence of several steps [1]. These include *i*) trapping of light and transfer of excitation energy, *ii*) electron transfer in the reaction center and charge separation, prevention of back electron transfer through sequential transfer of electrons, first to the primary quinone Q_A and then to a secondary quinone Q_B, *iii*) protonation of the secondary quinone Q_B, and *iv*) establishment of a proton gradient and synthesis of ATP. Prevention of back electron transfer is very essential for the progress of the reaction, and nature does it very efficiently through the sequential electron transfer to the quinones.

In the case of D–B–A systems, two strategies were employed for efficient charge separation. One of these involves the use of fullerene heteroaromatic dyads and tune the electron transfer process as a function of the donor strength. According to *Marcus*'

theory [18], the electron transfer rate increases with increasing exergonicity (normal region), reaches a maximum, and then decreases for very negative values of $-\Delta G^{\circ}$ (inverted region). By choosing dyad systems in which the exothermic forward electron transfer is located in the normal region of the *Marcus* curve and the back electron transfer process in the inverted region of the *Marcus* parabola, one can reduce the back electron-transfer rates and thereby ensure efficient charge separation. Certain fullerene substituted-aniline/heteroaromatic dyads were employed for this purpose.

Fullerene Substituted-Aniline/Heteroaromatic Dyads. – Although there are several reports in the literature on the design and studies of fullerene-based dyads, no major efforts have been made to investigate photoinduced intramolecular electron-transfer processes as a function of the donor strength. Heteroaromatic groups such as 10-methylphenoxazine and 10-methylphenothiazine are reported to be excellent electron donors in photoinduced electron-transfer reactions due to their low ionization potential and the ability to form extremely stable radical cations. Two series of fullerene-based dyads containing donor groups of varying oxidation potentials were used for these studies. The first series consists of fullerene-based dyads possessing heteroaromatic groups such as phenoxazine and phenothiazine as donors, whereas the second group consists of substituted anilines such as *p*-anisidine and *p*-toluidine as donor groups. Representative examples **4**–**7** are shown below [19].

The distance of separation between the donor and acceptor groups in these cases is kept more or less constant by using the same bridging unit. The free energy of charge separation in these systems mainly depends on the oxidation potential of the donor groups. The reported values ($E_{1/2}$ *vs.* SCE) in MeCN for *N*-methylphenoxazine, *N*-methylphenothiazine, *N*,*N*-dimethyl-*p*-anisidine, and *N*,*N*-dimethyl-*p*-toluidine are 329, 423, 490, and 650 mV, respectively. The electron-transfer processes in the second series are compared with a fullerene–aniline dyad **1**, possessing the same bridging unit (oxidation potential $E_{1/2}$ *vs.* SCE of *N*,*N*-dimethylaniline is 810 mV in MeCN).

The synthesis of the fullerene–heteroaromatic dyads **4** and **5**, as well as fullerene-aniline dyads **6** and **7** was achieved through the 1,3-dipolar cycloaddition of the corresponding azomethine ylides with C_{60}.

Molecular-modeling studies by the *Sybyl* force-field method suggest that the energy-minimized conformations of the fullerene–heteroaromatic dyads **4** and **5** as well as those of fullerene–*p*-anisidine and fullerene–*p*-toluidine dyads, **6** and **7**, respectively, are the extended ones. In the case of fullerene–heteroaromatic dyads, the edge-to-edge distance between the heteroaromatic N-atom and C_{60} is found to be 9.95 Å for **4** and 9.96 Å for **5**. The edge-to-edge distance between the aniline N-atom and C_{60} is found to be nearly the same (9.5 Å) for the fullerene–*p*-anisidine and fullerene–*p*-toluidine dyads, **6** and **7**, respectively and for the unsubstituted fullerene–aniline dyad **1**.

The visible absorption spectral features of the fullerene–heteroaromatic dyads **4** and **5** as well as the fullerene–*p*-anisidine and fullerene–*p*-toluidine dyads, **6** and **7**, respectively, are similar to that of the fullerene-aniline dyad **1**. The emission properties of the fullerene–heteroaromatic dyads **4** and **5**, and those of the fullerene–*p*-anisidine and fullerene–*p*-toluidine dyads, **6** and **7**, respectively, were found to be similar to those of the model pyrrolidine **3**.

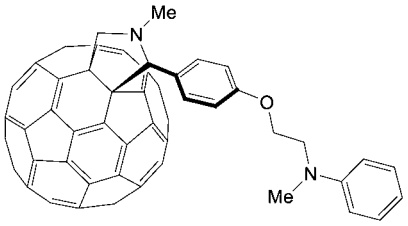

1

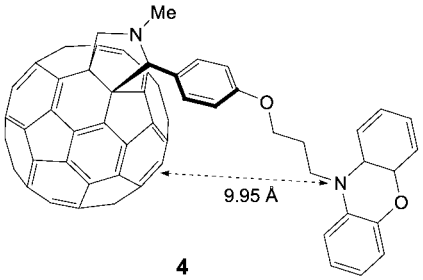

4

(329 mV $E_{1/2}$ *vs.* SCE)

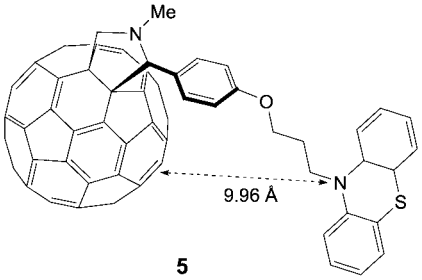

5

(423 mV $E_{1/2}$ *vs.* SCE)

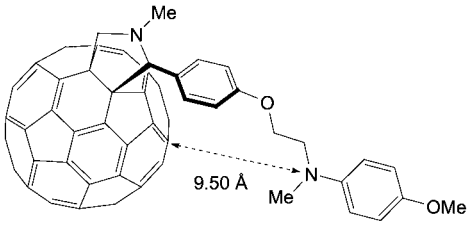

6

(490 mV $E_{1/2}$ *vs.* SCE)

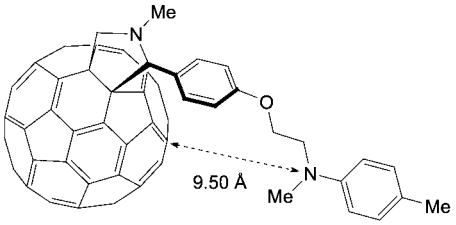

7

(650 mV $E_{1/2}$ *vs.* SCE)

The rate constants and quantum yields for charge separation (k_{CS} and ϕ_{CS}) *via* excited singlet states of the dyads were estimated from the corresponding fluorescence quantum yield of the dyad (ϕ_f), and the quantum yield and lifetime of the model compound (ϕ_{ref} and τ_{ref}, resp.), according to *Eqns. 1* and *2*.

$$k_{cs} = [(\phi_{ref}/\phi_f) - 1]1/\tau_{ref} \quad (1)$$

$$\phi_{cs} = k_{cs}/[(1/\tau_{ref}) + k_{cs}] \quad (2)$$

The rate constants and quantum yields for charge separation for the fullerene–heteroaromatic dyads **4** and **5**, and the fullerene–aniline dyads **6** and **7** are presented in

Table 2. A substantial decrease in fluorescence quantum yield was observed for all the dyads in polar solvents. In polar solvents, the free-energy changes for photoinduced electron-transfer are highly exothermic, and the electron-transfer process is thermodynamically allowed.

Table 2. *Fluorescence Quantum Yield, Rate Constant, and Quantum Yield of Charge Separation in Fullerene Heteroaromatic Dyads* **1** *and* **4**–**7**

Dyad	Toluene ($\varepsilon = 2.38$)		CH_2Cl_2 ($\varepsilon = 8.93$)		Benzonitrile ($\varepsilon = 25.20$)	
	ϕ_f [10^{-4}]	k_{CS} [10^9 s^{-1}][a]) (ϕ_{CS})[b])	ϕ_f [10^{-4}]	k_{CS} [10^9 s^{-1}][a]) (ϕ_{CS})[b])	ϕ_f [10^{-4}]	k_{CS} [10^9 s^{-1}][a]) (ϕ_{CS})[b])
4	3.5	0.56 (42%)	2.0	1.56 (67%)	1.8	1.85 (70%)
5	4.8	0.20 (20%)	2.5	1.11 (42%)	2.0	1.56 (47%)
6	2.6	1.09 (47%)	1.3	3.01 (78%)	1.2	3.13 (80%)
7	4.9	0.19 (18%)	2.3	1.34 (62%)	1.8	1.85 (62%)
1	6.8	–	3.3	0.64 (45%)	3.1	1.11 (49%)

[a]) $k_{CS} = [(\phi_{ref}/\phi_f) - 1]1/\tau_{ref}$. [b]) $\phi_{CS} = k_{CS}/[(1/\tau_{ref}) + k_{CS}]$.

Relatively large values of rate constants (k_{CS}) and quantum yields of electron transfer (ϕ_{CS}) observed from the singlet excited state are indicative of a rapid deactivation of the singlet excited state. The decrease in fluorescence yield arises from the reductive quenching of the fullerene singlet excited state by an electron transfer from the appended donor group. The deactivation of singlet excited site was accelerated with increasing solvent polarity for all dyads. On the other hand, deactivation rates, in a given solvent, were dependent on the oxidation potential of the donor group.

Nanosecond flash-photolysis experiments of the dyads were carried out by probing the transients absorbing in the UV/VIS-near-IR (350–1100 ns) region, for elucidating the mechanistic and kinetic details of the intramolecular electron transfer process [19]. Although the photoinduced electron transfer in fullerene-based systems is thermodynamically favorable due to the ionization potential of the donor groups, the solvent polarity can play a major role in the stabilization of the electron-transfer products.

The transient absorption spectrum of the phenothiazine dyad **5** in benzonitrile (*Fig. 2*), for example, shows two absorption maxima in the VIS region (450 and 520 nm) and another one in the near-IR region (λ_{max} at 1000 nm). It is evident that the transient spectra obtained in benzonitrile solution and in toluene exhibit distinctly different features. The bands in the VIS region (450 and 520 nm) are assigned to the radical cation of phenothiazine, whereas the band with the maximum around 1000 nm is assigned to C_{60} radical anion. The fate of the electron-transfer product was followed by monitoring the absorption-time profile at 520 and 1000 nm. Both these decays exhibit mono-exponential decay with a rate constant of 3.90×10^6 s^{-1}, which is the rate of charge recombination (k_{CR}).

Similar observations were made in the case of fullerene–phenoxazine dyad **4**, as well as fullerene–(*p*-substituted)aniline dyads **6** and **7**, following 337-nm laser pulse excitation. The back-electron-transfer rate constant for dyads **4**–**7** are in the range of $(2.4–3.9) \times 10^6$ s^{-1}.

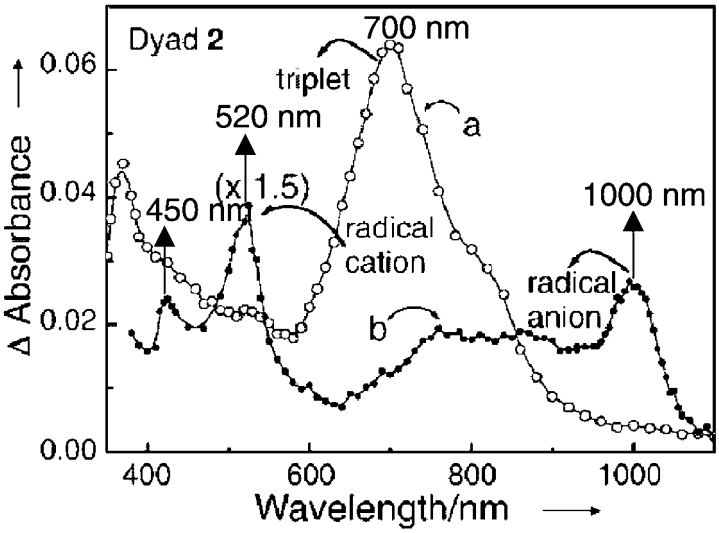

Fig. 2. *Difference absorption spectra, recorded following 337-nm laser pulse excitation of the fullerene–phenothiazine dyad* **5** (*ca.* 30 μM) *in deoxygenated toluene* (*a*) *and benzonitrile* (*b*) *in the VIS-NIR region.* The spectra were recorded at a delay of 200 ns (reprinted from [19] with permission from *Wiley-VCH*).

In general, one of the promising features of fullerene-based donor systems is their relatively slow k_{CR}. The rate constants for charge separation (k_{CS}) and charge recombination (k_{CR}) for the dyads **4**–**7** are shown in *Table 3*. It is evident that in dyads **4**–**7**, the back electron transfer is significantly slower than the forward electron transfer. These results can be explained in terms of an inverted region effect of the *Marcus* relationship in which the back electron transfer rate constants (k_{CR}) decrease gradually with an increase in the free energy changes ($-\Delta G_{CR}$).

Table 3. *Rate Constants for Charge Separation* (k_{CS})[a]) *and Charge Recombination* (k_{CR})[b]) *of Dyads* **4**–**7** *in Benzonitrile*[c])

Dyad	τ [ps]	k_{CS} [10^9 s^{-1}][a])	k_{CR} [10^6 s^{-1}][b])	k_{CS}/k_{CR}
4	375	2.00	2.99	699
5	450	1.56	3.90	400
6	254	3.27	3.39	964
7	380	1.97	2.43	810

[a]) Determined from the decay of the fullerene singlet state using ps transient absorption studies and from the relation: $k_{CS} = 1/\tau_{dyad} - 1/\tau_{ref}$ with τ_{ref} being the fullerene singlet-excited-state lifetime. [b]) Determined from the transient decay at 1000 nm using ns transient absorption studies. [c]) Fullerene singlet-excited-state lifetime is 1.5 ns.

The k_{CS} values were measured directly from picosecond transient absorption studies and also determined from fluorescence quantum yields. The exothermic forward

electron transfer is located in the normal region of the *Marcus* curve, *i.e.*, the unimolecular rate constant increases with increasing $-\Delta G_{CS}$. In summary, high ratios of k_{CS}/k_{CR} were achieved in the fullerene-substituted-aniline/heteroaromatic dyads. Thus, it is possible to tune the rates of electron transfer in these systems by varying the oxidation potentials of the donor groups linked to C_{60}.

Fullerene Clusters. – Another way of charge stabilization and slowing down the back electron reaction is by charge delocalization through fullerene clusters. Fullerenes and their derivatives are known to form clusters in mixed solvents that are optically transparent and thermodynamically stable. Recent studies have shown that fullerene-based cluster systems possess interesting photophysical and photochemical properties [20]. The photophysical and photochemical behaviors of the monomer and cluster forms of a bis- and tris-fullerene derivative have been examined to understand the factors that influence charge stabilization in these clusters.

The fullerene derivatives **8**–**10** that were examined are shown below. The mono-(C_{60}) was prepared through the reaction of an azomethine ylide, generated from 1,2,3-triphenylaziridine with C_{60} [8a]. The syntheses of both bis-(C_{60}) and tris-(C_{60}) have been achieved through the pathways similar to those of **1** and other dyads, reported earlier [8b][21].

The absorption spectra of bis-(C_{60}) and tris-(C_{60}), **9** and **10**, respectively, are characteristic of the mono-(C_{60}) derivative **8**. In mixed polar/non-polar solvents (*e.g.*, MeCN and toluene), however, these fullerenes readily form transparent clusters. These clusters exhibit broad featureless spectra, with increased molar extinction coefficients. These clusters are quite stable at room temperature and can be reverted back to the corresponding monomeric forms, on increasing the fraction of the nonpolar solvent (toluene).

The emission spectra of the monomer and cluster forms of bis-(C_{60}) and tris-(C_{60}), **9** and **10**, respectively, show characteristic emission bands with a maximum centered around 715 nm, which is similar to that of the monofunctionalized fullerene derivative [21]. The similarity of the absorption and emission features of **9** and **10** with those of **8** indicates that the individual fullerene moieties maintain their identity in displaying the excited-state properties.

Both bis-(C_{60}) and tris-(C_{60}), **9** and **10**, respectively, exhibit an additional shoulder around 775 nm in the emission spectra [21]. This band is particularly more prominent in **9**. The new shoulders observed in **9** and **10** are likely to arise from intramolecular interaction between the two excited fullerene moieties. Preliminary studies indicate that the relative intensities of both these bands are unaffected in the temperature range of 5–40° and solvent polarity (toluene to benzonitrile). The excitation spectra of **9**, recorded by monitoring the emission at 710, 740, and 775 nm, show similar spectral features that correspond to the absorption spectrum of the monomeric form **8**. Further studies are necessary to fully understand the dual emission behavior of such oligofullerenes.

A bathochromic shift (15–35 nm) in the emission maximum was observed for the clusters of bis-(C_{60}) and tris-(C_{60}) fullerene derivatives, **9** and **10**, respectively, in toluene/MeCN. The emission maximum in both **9** and **10** is observed around 750 and 735 nm, respectively [21]. The prominent red-shifted band around 750 nm of these

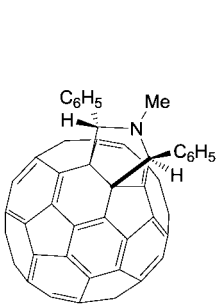

8

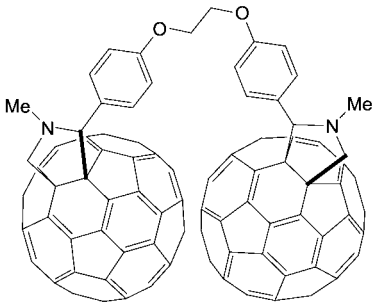

9

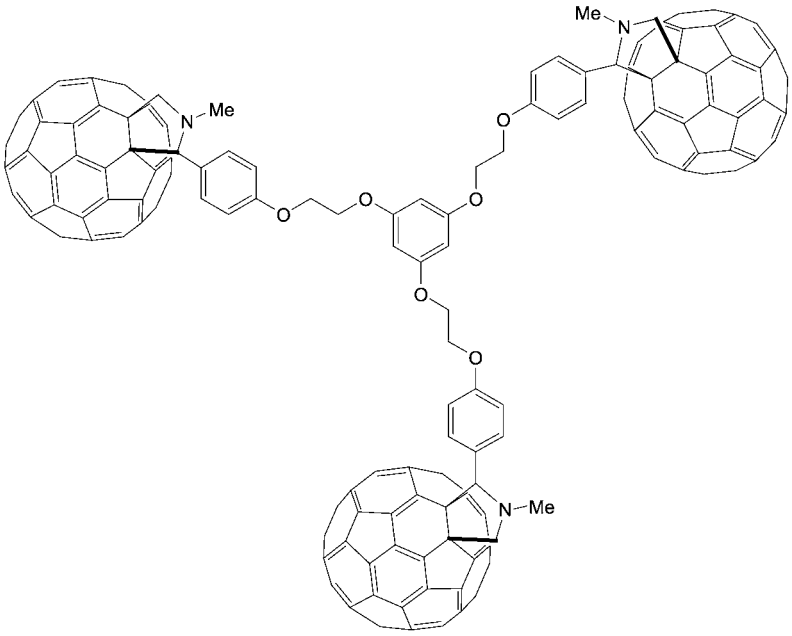

10

clusters confirms that they continue to exhibit photophysical properties similar to their monomer analogs.

Cluster-Size Analysis. – The clusters of bis-(C_{60}) and tris-(C_{60}) derivatives, **9** and **10**, respectively, were characterized by dynamic light-scattering method. The maximum cluster diameter for **9** and **10** were found to be 1.5 μm and 150 nm, respectively (*Fig. 3*, *A*). Both of these clusters showed a wide range of cluster-size distribution. The size distribution of tris-(C_{60}) clusters in MeCN/toluene is much narrower than that of

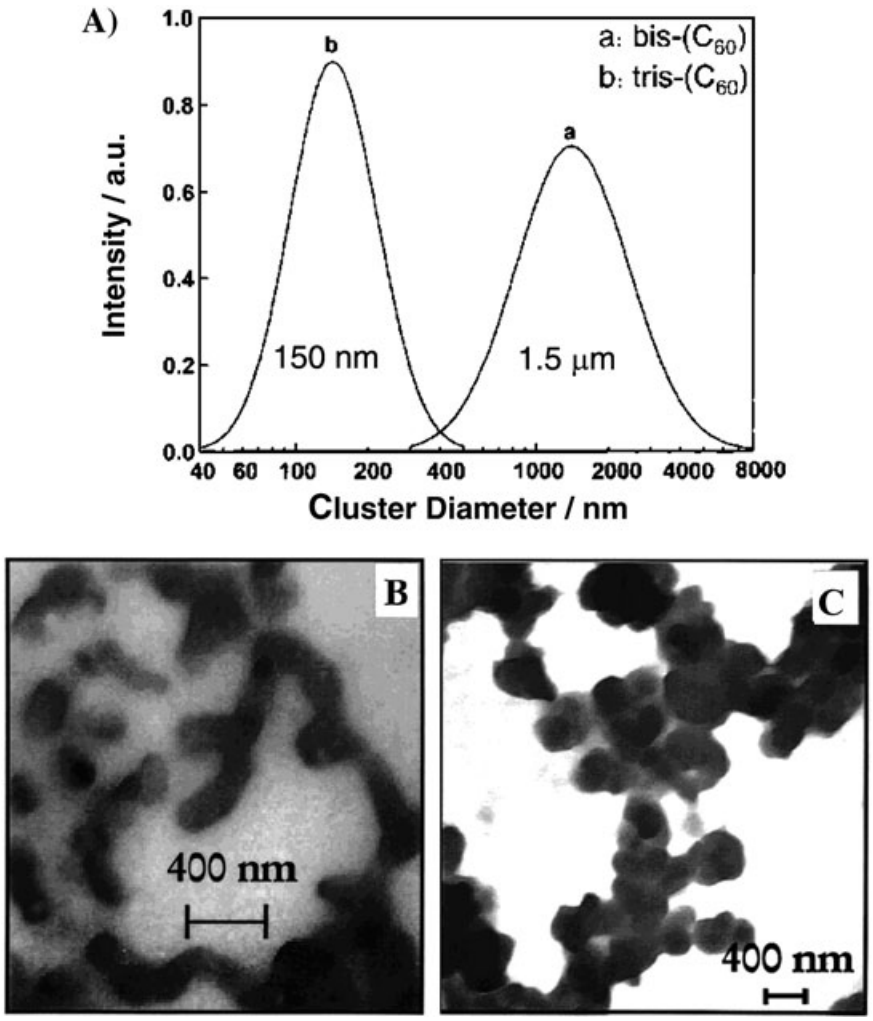

Fig. 3. A) *Dynamic light-scattering measurements indicate the average cluster diameter to be in the range of 100 nm to 1.5 μm.* B) *Clusters deposited on a carbon grid; elongated rods of varying lengths 200 nm to 1 μm.* C) *The globular clusters* (diameter *ca.* 100–400 nm) *are further linked to form a network of clusters* (reprinted from [21] with permission from the *American Chemical Society*).

bis-(C_{60}). Since the fullerene moieties are hydrophobic, they tend to self-aggregate to minimize their exposure to polar media.

The TEM (transmission electron microscopy) images of the clusters of bis-(C_{60}) and tris-(C_{60}) [21], **9** and **10**, respectively, prepared from MeCN/toluene mixture are shown in *Figs. 3*, *B* and *3*, *C*. The clusters of **10** are spherical in shape with diameters ranging from 100 to 400 nm. It is noticed that the self-assembled clusters of **10**, which are

globular in shape are further linked to form a network of clusters. Such self-assembly of clusters has been observed in thiol functionalized gold nanoparticles.

A different type of clustering has been observed in the case of bis-(C_{60}) clusters prepared in MeCN/toluene mixture. The clusters deposited on a carbon grid show elongated wire or rod-type structures of varying lengths (200 nm to 1 μm). These unusually elongated shapes explain the high dispersity observed for bis-(C_{60}) cluster suspension in the dynamic light-scattering experiments. Although the exact nature of interaction leading to the elongated structures is yet to be understood, it is evident that the linear stacking of molecules is preferred over three-dimensional clustering during the aggregation process in the case of bis-(C_{60}) clusters.

Aggregation of tris-(C_{60}) **10** on the other hand, has a geometric possibility to form clusters in a three-dimensional fashion. It is evident from TEM pictures that the tris-(C_{60}) derivative aggregates uniformly in all directions *via* hydrophobic interactions to give spherical structures. In both cases, the linker groups containing polar N- as well as O-atoms may preferably be exposed to the polar solvent environment.

A pictorial representation of the linear and three-dimensional modes of clustering in the case of bis-(C_{60}) **9** and tris-(C_{60}) **10**, respectively, is shown in *Fig. 4* [21].

Molecular-modeling calculations of bis-(C_{60}) and tris-(C_{60}) derivatives, **9** and **10**, respectively, were carried out with *Titan* software. The equilibrium geometrics were estimated by semiempirical AMI calculation. The energy-minimized conformations of **9** and **10** are shown in *Fig. 5*. The distance of separation between the two C_{60} moieties is found to be 5.6 Å for **9**. Such an energy-minimized structure favors a linear stacking, as the adjacent fullerene moieties interact to produce elongated clusters. On the other hand, the three fullerene moieties in **10**, are well separated from each other at distances of 15.9, 17.7, and 21.9 Å. The spatial arrangement of these fullerene moieties favors the three-dimensional packing, as the intermolecular interaction between fullerene moieties becomes favorable in all directions. Thus, we expect a spherical shaped clustering behavior for **10**.

It may be recalled that organic chromophores are known to undergo different types of well-defined aggregation (H, J, and herring-bone type) based on the nature of interacting molecules and the medium. The examples presented in this work demonstrate the ability to design different carbon nanostructures by simply modifying the fullerene functionalization. A template-driven clustering can further aid in defining the shape and size of these clusters. In addition, by attaching a specific redox-active or photoactive functional group to the fullerene moiety, it should be possible to design and tailor the properties of such clusters.

Excited-State Behavior of Bis-(C_{60}) and Tris-(C_{60}). – Singlet and triplet excited states of bis-(C_{60}) and tris-(C_{60}) derivatives, **9** and **10**, respectively, were probed by transient absorption spectroscopy. Picosecond transient absorption spectra of **9** in toluene (λ_{ex} 355 nm), for example, showed the formation of the singlet excited state with characteristic absorption in the 800–900-nm region. As the singlet excited state decayed, the growth of absorption in the 700-nm region due to the triplet was observed. Both **9** and **10** exhibit a lifetime of 1.25 ± 0.5 ns for the singlet excited state. The triplets of **9** and **10** absorb around 700 nm and have lifetimes in the range of 10–20 μs.

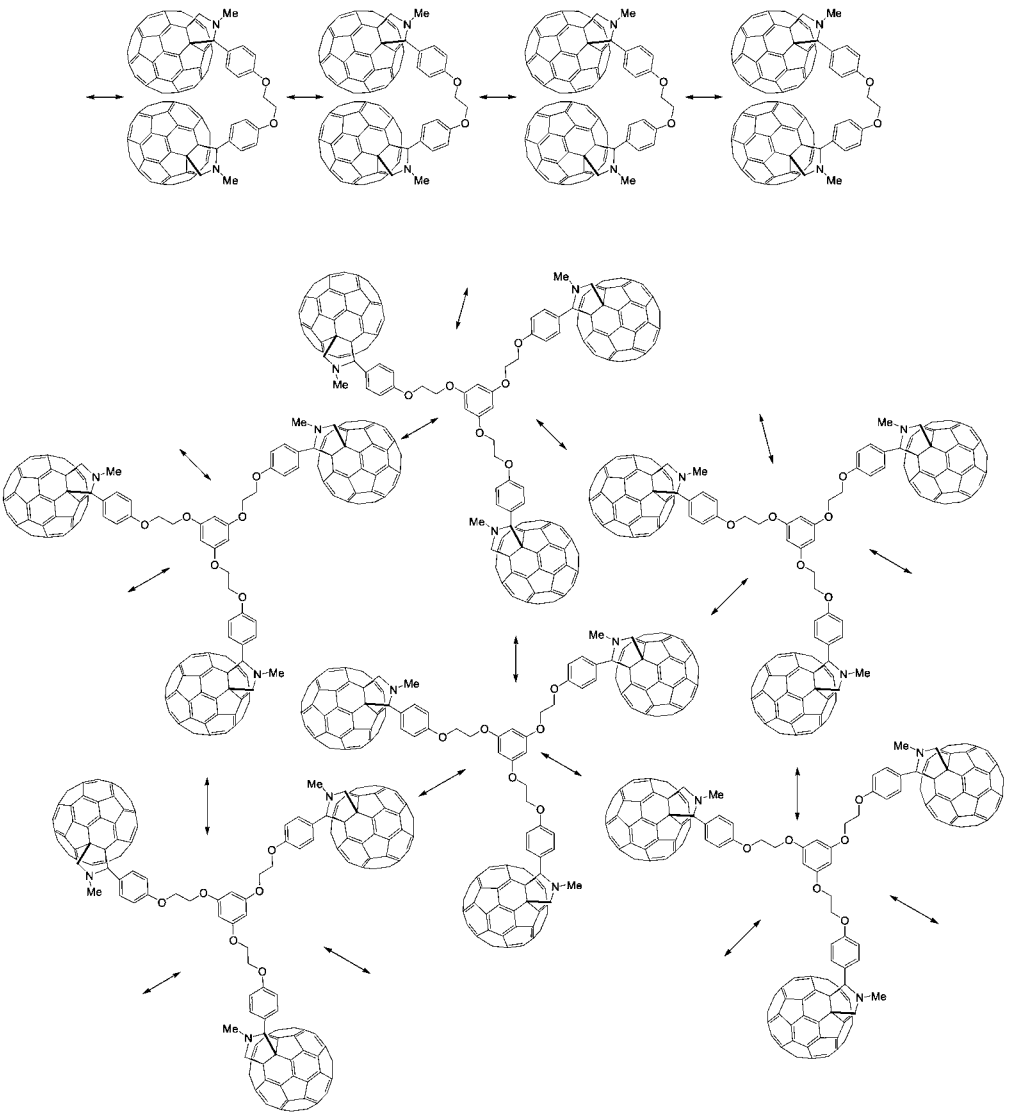

Fig. 4. *Preferred mode of clustering of bis-fullerene leading to linear growth and clustering of tris-fullerenes leading to spherical growth* (reprinted from [21b] with permission from the *Indian Academy of Sciences*).

Clusters of both **9** and **10** exhibit triplet–triplet absorption properties similar to those of the monomer form. For example, the triplet–triplet absorption spectrum of the clusters of **9** show an absorption maximum around 700 nm and has a lifetime of 11 μs in MeCN/toluene [21].

There have been several studies in recent years on inter- and intramolecular electron-transfer processes involving fullerenes and electron donors. In a recent

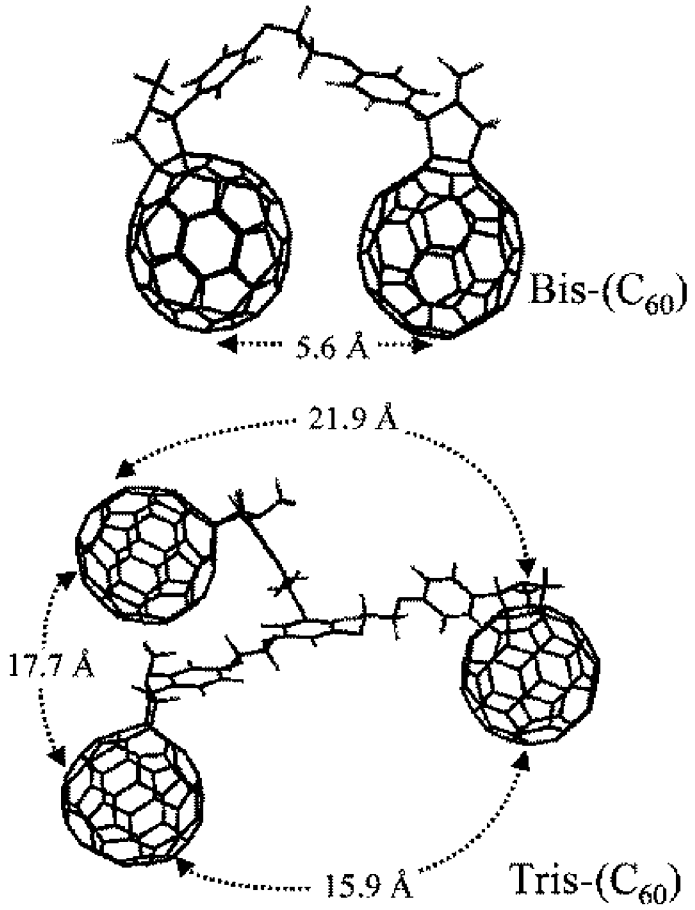

Fig. 5. *Energy-minimized conformations of bis-(C_{60}) and tris-(C_{60})* (reprinted from [21b] with permission from the *Indian Academy of Sciences*).

investigation [22], it was shown that charge stabilization occurs when intermolecular electron transfer is initiated by exciting the mono-(C_{60}) derivative (triphenyl-fullereno pyrrolidine) cluster in the presence of various electron donors. It was concluded from these studies that the close network of fullerene clusters facilitates the hopping of electrons, resulting in an increase in the spatial distance between the charge-separated radical ion pairs. It was of interest to examine whether the presence of multiple C_{60} units on the same C-backbone can bring about charge-stabilization effects, following the electron-transfer process. By employing *N*-methylphenothiazine (NMP) as an electron donor, the excited-state interactions as well as charge-stabilization properties of the bis-(C_{60}) and tris-(C_{60}) derivatives, **9** and **10**, respectively, were probed. The experimental procedure involved the addition of a known amount of NMP to MeCN solution, prior to the injection of the fullerene solution in toluene. This ensured the trapping of NMP within the network of the fullerene clusters.

It was observed that the fluorescence of **9** and **10** in the monomer and cluster forms is quenched by NMP, as the intermolecular electron-transfer process competes with the intersystem-crossing process. The bimolecular rate constants (k_q) estimated for the singlet excited state quenching of **9** and **10** were 5.5×10^9 and 5.3×10^9 $M^{-1}s^{-1}$, respectively.

Light-Induced Electron Transfer between Clusters of Bis-(C_{60}), and Tris-(C_{60}), and Electron Donors. – Using nanosecond-laser-flash photolysis, photoinduced electron transfer between bis-(C_{60}) and tris-(C_{60}) derivatives, **9** and **10**, respectively, and NMP was studied. The transient absorption spectra recorded for the monomer and cluster forms of **9** and **10** in presence of NMP showed similar features with absorption maxima at 520 nm due to $NMP^{\bullet+}$ and 1000 nm, due to fullerene anion.

The strong absorption of the fullerene anion at 1000 nm enables one to evaluate the fate of electron-transfer products by analyzing the absorption decay in monomer and cluster systems.

Charge Separation and Charge Stabilization. – The decay of the fullerene monomer anion depends on the number of fullerene units in the monomer and cluster forms. The decay of the monomer form of the fullerene anions could be fit to single-exponential decay, whereas biexponential kinetics was necessary to fit the cluster anions. Properties of the triplet excited states and fullerene anions of the fullerene derivatives under discussion are presented in *Table 4*.

Table 4. *Properties of the Triplet Excited States and Fullerene Anions*

Fullerene		Abs. max. triplet	Triplet lifetime	Abs. max anion	Anion lifetime[c] [μs]		Charge transfer quantum yield[d]
		[nm]	[μs]	[nm]	τ_1	τ_2	
Mono-(C_{60})	Monomer[a]	700	16.6	1010	18	–	0.11
	Cluster[b]	700	13.1	1010	16.6 (64%)	109 (36%)	0.13
Bis-(C_{60})	Monomer[a]	700	11.9	1000	20	–	0.09
	Cluster[b]	700	5.3	1000	11.8 (70%)	134 (25%)	0.07
Tris-(C_{60})	Monomer[a]	700	19.8	1000	34.0	–	0.11
	Cluster[b]	700	3.1	1000	12.0 (85%)	146 (15)	0.06

[a]) In toluene. [b]) In MeCN/toluene 19 : 1. [c]) Numbers in brackets indicate the fractional contribution to the overall decay. [d]) Measured from the fullerene anion yield ($\varepsilon(1000\ nm) = 16250\ M^{-1}\ cm^{-1}$) and benzophenone triplet as the actinometry reference ($\varepsilon(530\ nm) = 7600\ M^{-1}\ cm^{-1}$).

The fact that first-order decay kinetics is operative for the disappearance of the monomeric form of the fullerene anions suggests that the electron-transfer products exist within the close proximity of each other. Hence, the fast back electron transfer occurs mainly from close contact pairs and is not influenced by the diffusion of the two species within the bulk medium. On the other hand, in the cluster systems, one observes

the presence of two components. The faster component arises from the close-lying charge-separated pair, whereas the slower component involves the charge that is localized farther away from $NMP^{\bullet+}$ species. Thus, the clustering of fullerene moieties favors charge stabilization as the charge can quickly migrate from one fullerene moiety to another with ease. From the data presented in *Table 4*, it is evident that the fullerene anion lifetime increases with increasing number of fullerene moieties within the same cluster. Thus, an increase in the lifetime of 18 – 34 μs was observed for an increase in the number of fullerene units from one to three. These observations further support the argument that stabilization of charge can be achieved by bringing together several fullerene units in close proximity.

Conclusions. – Intramolecular and intermolecular electron transfer between excited fullerene and donor moiety results in the formation of electron-transfer products. The rate of electron-transfer efficiency of charge separation is dependent on the molecular configuration, redox potential of the donor, and the medium. Clustering the fullerene – donor systems provides a unique way to stabilize electron-transfer products. The stability of C_{60} anions in fullerene clusters opens up new ways to store and transport photochemically harnessed charges. Application of such systems in photochemical solar cells [23] and fuel cells [24] are already being explored. Since fullerene can undergo multiple reductions, the challenges lie ahead to store more than one electron per C_{60} moiety in electron-transfer processes.

This work was supported by the *Council of Scientific and Industrial Research*, Government of India, and the *Office of Basic Energy Science*, the *U.S. Department of Energy*. The authors thank Dr. *P. K. Sudeep* and Mr. *K. Yoosaf* for their help in preparing the manuscript. One of the authors (*M. V. G.*) thanks the *Jawaharlal Nehru Centre for Advanced Scientific Research*, Bangalore, India for financial support. This is contribution No. RRLT-PRU 198 from RRL, Trivandrum, and No. NDRL 4584 from the Radiation Laboratory.

REFERENCES

[1] J. Deisenhofer, H. Michel, *Angew. Chem., Int. Ed.* **1989**, *28*, 829; R. Huber, *Angew. Chem., Int. Ed.* **1989**, *28*, 848.

[2] J. S. Connolly, J. R. Bolton, in 'Photoinduced Electron Transfer, Part D', Eds. M. A. Fox, M. Channon, Elsevier, Amsterdam, 1988, p. 303; M. R. Wasielewski, in 'Photoinduced Electron Transfer, Part A', Eds. M. A. Fox, M. Channon, Elsevier, Amsterdam, 1988, p. 161; A. Osuka, S. Morikawa, K. Maruyama, S. Hirayama, T. Minami, *J. Chem. Soc., Chem. Commun.* **1987**, 359; M. A. Fox, in 'Photoinduced Electron Transfer III, Topics in Current Chemistry-159', Ed. J. Mattay, Springer, Berlin, 1991, p. 67; D. Gust, T. A. Moore, in 'Photoinduced Electron Transfer III, Topics in Current Chemistry-159', Ed. J. Mattay, Springer, Berlin, 1991, p. 103.

[3] H. Imahori, Y. Sakata, *Adv. Mater.* **1997**, *9*, 537; N. Martín, L. Sánchez, B. Illescas, I. Pérez, *Chem. Rev.* **1998**, *98*, 2527; 'Fullerenes and Related Structures', Ed. A. Hirsch, Springer, Berlin, 1999, Vol. 199; H. Imahori, Y. Sakata, *Eur. J. Org. Chem.* **1999**, *64*, 2445; F. Diederich, M. Gomez-Lopez, *Chem. Soc. Rev.* **1999**, *28*, 263; F. Diederich, R. Kessinger, *Acc. Chem. Res.* **1999**, *32*, 537; D. M. Guldi, *Chem. Commun.* **2000**, 321; D. M. Guldi, M. Prato, *Acc. Chem. Res.* **2000**, *33*, 695; D. Gust, T. A. Moore, A. L. Moore, *Acc. Chem. Res.* **2001**, *34*, 40; D. M. Guldi, N. Martín, *J. Mater. Chem.* **2002**, *12*, 1978; D. M. Guldi, *Chem. Soc. Rev.* **2002**, *31*, 22; Y.-P. Sun, in 'Molecular and Supramolecular Photochemistry', Vol. 1, Organic Photochemistry, Eds. V. Ramamurthy, K. S. Schanze, Marcel Dekker, New York, 1997, p. 325; C. S. Foote, in 'Topics in Current Chemistry, Electron Transfer 1', Ed. J. Mattay, Springer, Berlin, 1994, p. 347; P. V. Kamat, K.-D. Asmus, *Interface* **1996**, *5*, 22; F. Zhou, C. Jehoulelt, A. J. Bard, *J. Am. Chem. Soc.* **1992**, *114*, 11004; D. K. Dubois, K. M. Kadish, S. Flanagan, R. E. Haufler, L. P. E. Chibante, L. F. Wilsson, *J. Am. Chem. Soc.* **1992**, *114*,

3978; J. W. Arbogast, C. S. Foote, M. Kao, *J. Am. Chem. Soc.* **1992**, *114*, 2277; D. Gust, T. A. Moore, A. L. Moore, *J. Photochem. Photobiol. B* **2000**, *58*, 63.

[4] R. M. Williams, M. Koeberg, J. M. Lawson, Y.-Z. An, Y. Rubin, M. N. Paddon-Row, J. W. Verhoeven, *J. Org. Chem.* **1996**, *61*, 5055.

[5] D. Kuciauskas, P. A. Liddell, A. L. Moore, T. A. Moore, D. Gust, *J. Am. Chem. Soc.* **1998**, *120*, 10880; P. A. Liddell, D. Kuciauskas, J. P. Sumida, B. Nash, D. Nguyen, A. L. Moore, T. A. Moore, D. Gust, *J. Am. Chem. Soc.* **1997**, *119*, 1400; D. Kuciauskas, S. Lin, G. R. Seely, A. L. Moore, T. A. Moore, D. Gust, T. Drovetskaya, C. A. Reed, P. D. W. Boyd, *J. Phys. Chem.* **1996**, *100*, 15926; P. A. Liddell, J. P. Sumida, A. N. Macpherson, L. Noss, G. R. Seely, K. N. Clark, A. L. Moore, T. A. Moore, D. Gust, *Photochem. Photobiol.* **1994**, *60*, 537; H. Imahori, K. Hagiwara, M. Asoki, T. Akiyama, S. Taniguchi, T. Okada, M. Shirakawa, Y. Sakata, *J. Am. Chem. Soc.* **1996**, *118*, 11771.

[6] P. S. Baran, R. R. Monaco, A. U. Khan, D. I. Schuster, S. R. Wilson, *J. Am. Chem. Soc.* **1997**, *119*, 8363.

[7] a) D. M. Guldi, *Pure Appl. Chem.* **2003**, *75*, 1069; b) N. S. Sariciftci, F. Wudl, A. J. Heeger, M. Maggini, G. Scarrano, M. Prato, J. Bourassa, F. C. Ford, *Chem. Phys. Lett.* **1995**, *247*, 510.

[8] a) K. G. Thomas, V. Biju, M. V. George, D. M. Guldi, P. V. Kamat, *J. Phys. Chem. A* **1998**, *102*, 5341; b) K. G. Thomas, V. Biju, M. V. George, D. M. Guldi, P. V. Kamat, *J. Phys. Chem. B* **1999**, *103*, 8864.

[9] H. Imahori, K. Yamada, M. Hasegawa, S. Taniguchi, T. Okada, Y. Sakata, *Angew. Chem., Int. Ed.* **1997**, *36*, 2626.

[10] T. G. Linssen, K. Durr, M. Hanack, A. Hirsch, *Chem. Commun.* **1995**, 103.

[11] M. Maggini, D. M. Guldi, S. Mondini, G. Scorrano, F. Paolucci, P. Ceroni, S. Roffia, *Chem. – Eur. J.* **1998**, *4*, 1992.

[12] D. M. Guldi, M. Maggini, G. Scorrano, M. Prato, *J. Am. Chem. Soc.* **1997**, *119*, 974.

[13] R. M. Williams, J. M. Zwier, J. W. Verhoeven, *J. Am. Chem. Soc.* **1995**, *117*, 4093.

[14] C. Luo, M. Fujitsuka, A. Watanabe, O. Ito, L. Gan, Y. Huang, C.-H. Huang, *J. Chem. Soc., Faraday Trans.* **1998**, *94*, 527.

[15] K. G. Thomas, V. Biju, D. M. Guldi, P. V. Kamat, M. V. George, *J. Phys. Chem. A* **1999**, *103*, 10755.

[16] Sybyl force field method, PC SPARTAN, Wavefunction, Inc., 18401, Von Karman, Suite 370, Irvine, CA 92612.

[17] P. V. Kamat, T. W. Ebbesen, N. M. Dimitrijevic, A. J. Nozik, *Chem. Phys. Lett.* **1989**, *157*, 384.

[18] R. A. Marcus, *J. Chem. Phys.* **1956**, *24*, 966; R. A. Marcus, N. Sutin, *Biochim. Biophys. Acta* **1985**, *811*, 265

[19] K. G. Thomas, V. Biju, P. V. Kamat, M. V. George, D. M. Guldi, *Chem. Phys. Chem.* **2003**, *4*, 1299.

[20] Y.-P. Sun, C. E. Bunker, *Nature (London)* **1993**, *365*, 398; Y.-P. Sun, C. E. Bunker, *Chem. Mater.* **1994**, *6*, 578; Y.-P. Sun, B. Ma, C. E. Bunker, B. Liu, *J. Am. Chem. Soc.* **1995**, *117*, 12705; M. T. Beck, *Pure Appl. Chem.* **1998**, *70*, 1881; D. M. Guldi, H. Hungerbuhler, K.-D. Asmus, *J. Phys. Chem.* **1995**, *99*, 13487; S. Nath, H. Pal, D. K. Palit, A. V. Sapre, J. P. Mittal, *J. Phys. Chem. B* **1998**, *102*, 10158; A. Beeby, J. Eastoe, R. K. Heenan, *Chem. Commun.* **1994**, 173; Y. M. Wang, P. V. Kamat, L. K. Patterson, *J. Phys. Chem.* **1993**, *97*, 8793.

[21] a) V. Biju, P. K. Sudeep, K. G. Thomas, M. V. George, *Langmuir* **2002**, *18*, 1831; b) M. V. George, *Proc. Indian Acad. Sci.* **2003**, *115*, 225.

[22] V. Biju, S. Barazzouk, K. G. Thomas, M. V. George, P. V. Kamat, *Langmuir* **2001**, *17*, 2930.

[23] P. V. Kamat, S. Barazzouk, S. Hotchandani, K. G. Thomas, *Chem. – Eur. J.* **2000**, *6*, 3914; T. Hasobe, H. Imahori, S. Fukuzumi, P. V. Kamat, *J. Am. Chem. Soc.* **2003**, *125*, 14962; P. V. Kamat, M. Haria, S. Hotchandani, *J. Phys. Chem. B* **2004**, *108*, 5166; P. V. Kamat, K. G. Thomas, in 'Nanoscale Materials', Eds. L. M. Liz-Marizan, P. V. Kamat, Kulwer Academic Publishers, 2003, Chapt. 20, p. 475; J. L. Segura, N. Martin, D. M. Guildi, *Chem. Soc. Rev.* **2005**, 31.

[24] K. Vinodgopal, M. Haria, D. Meisel, P. V. Kamat, *Nano. Lett.* **2004**, *4*, 415.

Received January 20, 2005